RESEARCH ARTICLE

Prolonged Corticosterone Exposure Induces Dendritic Spine Remodeling and Attrition in the Rat Medial Prefrontal Cortex

Rachel M. Anderson, Ryan M. Glanz, Shane B. Johnson, Mary M. Miller, Sara A. Romig-Martin, and Jason J. Radley*

Department of Psychological and Brain Sciences and Program in Neuroscience, University of Iowa, Iowa City, Iowa 52242

ABSTRACT

The stress-responsive hypothalamo–pituitary–adrenal (HPA) axis plays a central role in promoting adaptations acutely, whereas adverse effects on physiology and behavior following chronic challenges may result from overactivity of this system. Elevations in glucocorticoids, the end-products of HPA activation, play roles in adaptive and maladaptive processes by targeting cognate receptors throughout neurons in limbic cortical networks to alter synaptic functioning. Because previous work has shown that chronic stress leads to functionally relevant regressive alterations in dendritic spine shape and number in pyramidal neurons in the medial prefrontal cortex (mPFC), this study examines the capacity of sustained increases in circulating corticosterone (B) alone to alter dendritic spine morphology and density in this region. Subcutaneous B pellets were implanted in rats to provide continuous exposure to levels approximating the circadian mean or peak of the steroid for 1, 2, or 3 weeks. Pyramidal neurons in the prelimbic area of the mPFC were selected for intracellular fluorescent dye filling, followed by high-resolution three-dimensional imaging and analysis of dendritic arborization and spine morphometry. Two or more weeks of B exposure decreased dendritic spine volume in the mPFC, whereas higher dose exposure of the steroid resulted in apical dendritic retraction and spine loss in the same cell population, with thin spine subtypes showing the greatest degree of attrition. Finally, these structural alterations were noted to persist following a 3-week washout period and corresponding restoration of circadian HPA rhythmicity. These studies suggest that prolonged disruptions in adrenocortical functioning may be sufficient to induce enduring regressive structural and functional alterations in the mPFC. J. Comp. Neurol. 000:000–000, 2016.

INDEXING TERMS: glucocorticoids; HPA axis; prelimbic; confocal laser-scanning microscopy; NeuronStudio

A hallmark of the mammalian stress response entails activation of the hypothalamo–pituitary–adrenal (HPA) axis, a neuroendocrine cascade that stimulates glucocorticoid secretion from the adrenal gland (Antoni, 1986). A substantial body of research suggests that the capacity of environmentally salient stimuli to activate the HPA axis depends on modulatory control from a network of limbic forebrain cell groups that coordinate physiological and behavioral responses for adaptive coping (Feldman and Conforti, 1980; Diorio et al., 1993; Herman et al., 1995; Jaferi and Bhatnagar, 2006). In rodents, the medial prefrontal cortex (mPFC) is exemplary in this regard, performing both cognitive operations important for behavioral adaptation and neuroendocrine adjustments under stressful conditions. The prelimbic area (PL) is a centrally located subfield within the mPFC that straddles two broad functional domains, with more dorsal- and ventral-lying regions issuing projections that access distinct neural circuitries to modulate limbic-cognitive and visceromotor functions, respectively (Sesack et al., 1989; Vertes, 2004;

Grant sponsor: National Institutes of Health; Grant number: MH-095972 (to J.J.R.); Grant sponsor: Brain & Behavior Research Foundation National Alliance for Research on Schizophrenia and Depression (to J.J.R.).

*CORRESPONDENCE TO: Dr. Jason Radley, Department of Psychology, University of Iowa, E232 Seashore Hall, Iowa City, IA 52242. E-mail: jason-radley@uiowa.edu

Received December 8, 2015; Revised March 31, 2016;
Accepted April 20, 2016.
DOI 10.1002/cne.24027
Published online Month 00, 2016 in Wiley Online Library (wileyonlinelibrary.com)

Gabbott et al., 2005). The PL exhibits robust structural and functional plasticity in response to a variety of environmental stimuli and experiences, thus increasing its repertoire of response capabilities under changing contexts, such as chronic stress. Whereas glucocorticoids have widespread effects on prefrontal functions relevant for adaptation during acute challenges (Shors et al., 1992; McIntyre et al., 2003; Yuen et al., 2009), perturbations in HPA activity following prolonged stress are associated with maladaptive changes in many of these responses (Mizoguchi et al., 2000; Hains et al., 2009; Hinwood et al., 2012; McKlveen et al., 2013; Radley et al., 2013).

Evidence from our laboratory and others has shown that chronic stress is associated with structural remodeling of dendritic spines in mPFC pyramidal neurons and accompanying impairments in cognitive functioning (Liston et al., 2006; Radley et al., 2006, 2008, 2013), suggesting a role for altered adrenocortical activity in producing these changes. Although there is an extensive literature highlighting the capacity of glucocorticoids to alter hippocampal (Watanabe et al., 1992a; Watanabe et al., 1992b; McEwen, 1998; Sousa et al., 2000; Alfarez et al., 2009; Morales-Medina et al., 2009; Tanokashira et al., 2012; Wosiski-Kuhn et al., 2014) and amygdalar (Vyas et al., 2002, 2006; Mitra et al., 2005; Mitra and Sapolsky, 2008; Grillo et al., 2015) plasticity, information regarding glucocorticoid effects on structural plasticity in the mPFC has not been as forthcoming. Evidence that prolonged elevations in glucocorticoids induce regressive dendritic spine alterations in mPFC (Liu and Aghajanian, 2008; Gourley et al., 2013) and related cortical areas (Liston and Gan, 2011; Liston et al., 2013) is contrasted by conflicting reports of either no change (Cerqueira et al., 2007) or increased dendritic spine density in the mPFC (Seib and Wellman, 2003). Another complicating factor in evaluating the available evidence is that much of it is derived from Golgi-based approaches that hamper visualization of small spines that make up ~50% of the total population (see, e.g., Dumitriu et al., 2011). Therefore, we critically examine the effects of continuous corticosterone (B) exposure on rat dendritic spine density and morphometric alterations in pyramidal neurons in the PL using a high-resolution three-dimensional (3D) analytic approach (Rodriguez et al., 2006; Radley et al., 2008). We show that continuous B exposure for at least 2 weeks induces enduring dendritic spine remodeling and loss in the PL that persists even after 3 weeks of restoration of normal HPA axis rhythmicity. These studies highlight a prominent role for alterations in the mPFC that may result from repeated stress exposure or other contexts, such as Cushing's syndrome or aging.

MATERIALS AND METHODS

Animals

The animals used in this study were 3-month-old male Sprague Dawley albino rats (Charles River Laboratories, Kingston, PA). Rats were housed singly and maintained on a 12-hour light/dark cycle (lights on at 0600 hours) with free access to food and water. All experimental protocols were approved by the institutional animal care and use committee of the University of Iowa.

Glucocorticoid treatment regimens

Experiment 1: effects of varying doses of B on structural plasticity in the PL

Rats were adrenalectomized and implanted with slow-release B pellets (i.e., 100 and 200 mg) to clamp circulating levels of this hormone to that of either the circadian mean (~9 μg/dl) or the peak (~14 μg/dl; see Results) over a 2-week period for the assessment of structural plasticity effects in PL neurons. The decision to perform adrenalectomies in groups of rats receiving constant B was based on the desire to provide an independent assessment of B pellet efficacy that may otherwise be masked by endogenous adrenocortical activity in an intact animal. Rats were anesthetized with isoflurane and adrenalectomized by the dorsal approach. In the same surgical procedure, adrenalectomized rats were implanted subcutaneously in the interscapular region with 100-mg (n = 9) or 200-mg (n = 15) B pellets that provided a constant and slow release into the general circulation for 3 weeks (Innovative Research of America, Sarasota, FL). An additional group of rats received a sham adrenalectomy (ADX; n = 21), which involved all of the same procedural steps except removal of the adrenal gland, and were then implanted with inert cholesterol pellets of weight equal to the B pellets. On day 14, B pellet efficacy and baseline adrenocortical activity in B-replaced and sham rats, respectively, were confirmed by collection of repeated blood samples at AM and PM times and radioimmunoassay of B, and all rats were perfused on the morning of day 15.

Experiment 2: persistence of B-induced structural alterations in the PL following a 3-week recovery period

To assess the persistence of glucocorticoid-induced alterations in PL neuronal architecture, this experiment involved replacement with high-dose B pellets (200 mg) spanning the 3-week duration of its release capability, followed by a 3-week recovery period (n = 14). Rats in these experiments were not adrenalectomized to allow for the normalization of circadian HPA activity through

the course of the 3-week recovery period. A second group of rats received the same treatment course of B (n = 12); however, their pellet implants were staggered to begin during the second 3-week period of the experiment so that the perfusion and cell loading procedures would be phase locked with the B + recovery group. A third group of rats received implantation of sham cholesterol pellets (n = 10), randomized between the first and second 3-week intervals to parallel procedures in the two groups of B-treated rats. On days 14 and 35, rats from all three groups were subjected to repeated AM and PM blood sampling for radioimmunoassay of plasma B levels. Pellet efficacy (on day 14) and normalization of HPA activity (on day 35) were assessed in the B + recovery group, whereas B efficacy and baseline adrenocortical activity were confirmed in B- and sham-implanted rats (days 35 and 14, respectively).

Experiment 3: effects of short-term B exposure on structural plasticity in the PL

To acquire information with respect to the temporal characteristics of glucocorticoid-induced alterations in the PL, dendritic spine morphology was examined in rats exposed to high-dose B (200 mg) compared with sham-implanted controls for 7 days (n = 12/group). B pellet efficacy and baseline adrenocortical activity in B-replaced and sham rats were confirmed by collection of repeated blood samples at AM and PM times and radioimmunoassay of B on day 5 of steroid exposure.

Blood collection and radioimmunoassay

Adrenocortical activity was assessed by obtaining blood from the tail vein of rats at 0700 and 1700 hours on the day of sampling. Previous work from our laboratory has shown that these time points of sampling correspond well with nadir AM and peak PM values of B secretory activity in adrenally intact rats. For blood collection, rats were restrained briefly (15–30 seconds), and a small longitudinal incision was made at the distal tip of the tail with a sterile blade. Blood samples (~200 μl) were collected into chilled plastic microfuge tubes containing EDTA and aprotinin, centrifuged, and fractionated for storage of plasma at −80 °C until assayed. Plasma B was measured without extraction with an antiserum raised in rabbits against a B-BSA conjugate and ^{125}I-B-BSA as tracer (MP Biomedicals, Santa Ana, CA). Assay sensitivity was 0.8 μg/dl; intra- and interassay coefficients of variance were 5% and 10%, respectively.

Histology and tissue processing

Rats were anesthetized with sodium pentobarbital (100 mg/kg, i.p.) and perfused via the ascending aorta with 100 ml 1% paraformaldehyde (PFA) and 0.125% glutaraldehyde in 0.1 M phosphate-buffered saline (PBS; pH 7.4), followed by 500 ml of 4% PFA and 0.125% glutaraldehyde in PBS at a flow rate of 55 ml/minute. After postfixation, the pregenual pole of the cortex was sectioned coronally into 250-μm-thick slabs with a VT-1000S oscillating tissue slicer (Leica, Wetzlar, Germany) and stored in 0.1 M PBS containing 0.1% sodium azide at 4 °C until the time of cell loading.

Intracellular dye injections

The procedures used in this experiment are from previous work by researchers who used the same methodology (Radley et al., 2006; Anderson et al., 2014). Coronal tissue slabs were treated in the DNA-binding fluorescent stain 4′,6-diamidino-2-phenylindole (DAPI; Invitrogen, Carlsbad, CA) to distinguish among nuclear lamination patterns that distinguish the PL from other adjacent-lying prefrontal cortical subfields. DAPI-treated sections were mounted on nitrocellulose filter paper and submerged in a tissue culture dish containing PBS and viewed under fluorescence with a DM5500 fixed-stage microscope (Leica). Injections of 5% Lucifer yellow (LY; Invitrogen) were administered by iontophoresis through micropipettes (1–2-μm inner diameter) under a DC current of 1–6 nA for 5–10 minutes. The placement of injections was evaluated with reference to standard cytoarchitectonic parcellations of the PL (Krettek and Price, 1977; Vogt and Peters, 1981). The regions are of primary interest for distinguishing the PL from the adjacent-lying regions, from dorsal to ventral, the dorsal subdivision of the anterior cingulate area (ACd), the PL, and the infralimbic area (IL). In DAPI-stained material, the ACd is characterized by a sparse layer 3 and a loosely packed and broad layer 5, which distinguishes it from the more homogeneous layer 5 and large, darkly stained cells that make up the PL. The distinction between the PL and the IL is allowed by the relatively indistinct lamination pattern that emerges ventrally and the irregular border between layers 1 and 3 that typify the IL.

In all three experiments, neurons in layers 2 and 3 the of the PL (corresponding to anteroposterior coordinates 2.9–3.5 mm relative to bregma) were selected for the dye injection procedure, whereas experiment 2 involved the selection of neurons in layers 2, 3, and 5. The general technique for cell filling involved carefully observing the passive diffusion of LY resulting from application of a negligibly small amount of current from the advancing micropipette tip at ×40; LY diffuses amorphously until hitting a dendritic process or cell body, at which time the dye becomes restricted intracellularly. After several neurons were filled

intracellularly, tissue sections were mounted on glass slides and coverslipped in Vectashield (Vector Laboratories, Burlingame, CA).

Dendritic morphologic analyses of PL neurons in layers 2 and 3

Neuronal reconstructions were performed for the analysis of quantitative changes in dendritic morphology as a function of the B treatment regimens employed. Apical dendrites of pyramidal neurons in layers 2 and 3 of the PL are morphologically heterogeneous and have been shown to retain relatively consistent quantitative indices (i.e., branch length, number of branch endings), which allows pooling them into a single analysis (Cook and Wellman, 2004; Radley et al., 2004; Liston et al., 2006; Cerqueira et al., 2007). On the other hand, because layer 5 neurons have highly contrasting morphological features (Larkman and Mason, 1990; Kasper et al., 1994; Tsiola et al., 2003; Holtmaat et al., 2006; van Aerde and Feldmeyer, 2015), the dendritic morphologic analyses performed in the current study were restricted to data sets (i.e., experiments 1 and 3) that encompassed neurons in layers 2 and 3 only.

An experimenter unaware of the treatment condition for each animal performed neuronal reconstructions and data analyses. Pyramidal neuron dendritic arbors in layers 2 and 3 of the PL were reconstructed in 3D with a computer-assisted morphometry system consisting of a DM4000R (Leica) equipped with an MS-2000 XYZ computer-controlled motorized stage (Applied Scientific Instrumentation, Eugene, OR), QImaging (Surrey, British Columbia, Canada) Blue digital camera, Dell computer, and morphometry software (MBF Bioscience, Williston, VT). Neurons were visualized, and the dendritic tree was reconstructed with a Leica Apochromat $\times 40$ objective with a numerical aperture (NA) of 1.4 in Neurolucida software (RRID:SCR_001775; MBF Bioscience). To be considered for dendritic morphologic analysis, LY-filled PL neurons had to exhibit complete filling of the arbor as evidenced by well-defined endings and a minimum amount of truncated branches. Optimal cases involved apical dendritic trajectories that generally coursed parallel to or gently downward from the top surface of the section. Truncations in apical dendrites were permitted only in instances in which collateral branches were deemed to be nearing the point of termination or unable to make any further bifurcations. For basal dendrites, it was common to retain an average of one to three entirely intact arbors for a given LY-filled neuron, such that analyses on intact branches were performed for this category. Total length (in micrometers) and number of branch endings for apical and basal dendrites were obtained from each neuronal reconstruction and analyzed as described below.

Confocal laser scanning microscopy and dendritic spine analysis

2D renderings for each neuron were obtained in Neurolucida from the neuronal reconstruction procedures described above, and a radial distance of 150 μm from the soma was selected as a boundary delineating proximal and distal portions of the dendritic tree. Within these regions, branches were randomly selected for imaging from each neuron for an average of three segments per neuron and five neurons for each animal. The selection criteria for confocal imaging of dendritic segments were based on previous reports (Radley et al., 2006, 2013; Anderson et al., 2014) and required that segments 1) possess a diameter of <3 μm because larger diameter dendrites in PL pyramidal neurons exhibit greater variability in spine density values, 2) reside within a depth of 70 μm from the top surface of the section because of the limited working distance of the optical system, 3) either be parallel to or course gently relative to the coronal surface of the section (i.e., this helps to minimize z-axis distortion and facilitate the unambiguous identification of spines), and 4) have no overlap with other branches that would obscure visualization of spines. In contrast to the dendritic arborization analyses described above, dye-filled neurons containing truncated branches were permissible for their inclusion into the dendritic spine imaging and analysis as long as they exhibited complete filling of the dendritic arbor and well-defined branch tips. z-Stacks were collected on a Leica SP5 confocal laser scanning microscope equipped with an argon laser and a $\times 100$, 1.4 NA oil-immersion objective, with voxel dimensions of $0.1 \times 0.1 \times 0.1\ \mu m^3$. Settings for pinhole size (one airy disc), gain, and offset were initially optimized and then held relatively constant throughout the study to ensure that all images were digitized under similar illumination conditions at a resolution of 512×512 pixels. Images were deconvolved with AutoDeblur (Media Cybernetics, Silver Spring, MD), and spine analyses were performed in the semiautomated software NeuronStudio (RRID:SCR_013798; Computational Neurobiology and Imaging Center; http://research.mssm.edu/cnic/tools-ns.html; Rodriguez et al., 2006, 2008, 2009; Radley et al., 2008; Anderson et al., 2014), which analyzes dendritic length, spine density, and morphometric features (i.e., head/neck diameter, volume, subtype) in 3D for each dendritic spine. Spines were classified as thin or mushroom shaped if the ratio of the head diameter to neck

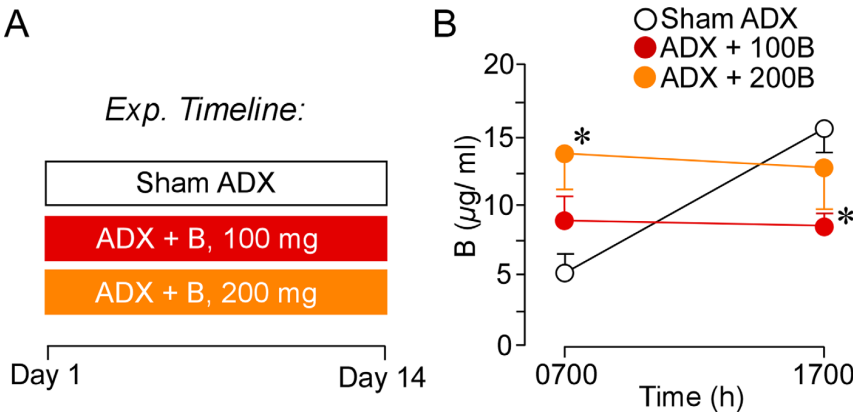

Figure 1. **A**: Time line of the first experiment. On day 1, animals underwent ADX surgeries and B pellet implantation or sham ADX and cholesterol pellet implantation. On day 14, blood was collected to assay for effectiveness of pellet increasing B levels. **B**: Graph depicting mean ± SEM plasma B levels at AM and PM sampling of B as a function of treatment group. These data reveal that 200-mg B (200B) pellets clamp levels to peak circadian levels, whereas 100-mg B (100B) pellets clamp B levels to values approximating the circadian mean. Control, n = 10; 100B and 200B, n = 6. $^*P < 0.05$, significantly different from sham-treated animals.

diameter was >1.1. If their ratio exceeded this value, spines with a maximum head diameter >0.4 μm were classified as mushroom shaped; otherwise, they were classified as thin. Spines with head-to-neck diameter ratios < 1.1 were also classified as thin if the ratio of spine length to neck diameter was >2.5; otherwise, they were classified as stubby. A fourth category, filopodial spines, exhibited a long and thin shape, with no enlargement at the distal tip. Because these were observed very seldom, they were classified as thin subtypes. Finally, data readouts from the spine analysis algorithm were visually compared by the experimenter for each optical stack to verify accurate subtype classifications for dendritic spines.

Statistical analysis

Group data from the B radioimmunoassay were compared by repeated-measures ANOVA, followed by pairwise comparisons with Fisher's least significant difference (LSD) at both morning and evening times. Data are expressed as mean ± SEM. Dendritic branch and spine morphometric data are averaged from each animal (i.e., three to five segments/neuron, five to seven neurons/rat) as a function of treatment. The final group sizes in both experiments are lower than our starting sample sizes reported above. This difference is due to the fact that the success rate from perfused rats that yield suitable numbers of fluorescent dye-filled neurons for inclusion into the analysis was ~55%. The effects on overall dendritic length, number of branch endings, and dendritic spine and subtype densities were compared by one-way ANOVA. Population analysis of spine volume as a function of subtype and experimental treatment were analyzed via comparison of cumulative frequency distributions with the Kolmogorov-Smirnov (K-S) test in Matlab (MathWorks, Natick, MA). Additional correlational tests were performed to determine whether each dependent measure varied as a function of integrated B values for each subject; however, because no significant trends were identified, these results are not reported here. All pairwise comparisons were made with Fisher's LSD with significance set at $P < 0.05$, and data are expressed as mean with SEM. Significance for the K-S test was set at $P < 0.01$.

RESULTS

Experiment 1: effects of varying doses of B on structural plasticity in the PL

Characterization of plasma B levels

Two weeks after pellet implantation (i.e., 100 mg, 200 mg, or cholesterol), blood samples were collected from the tail vein of rats at times approximating the circadian nadir (0700 hours) and zenith (1700 hours), determined from our previous characterization of the sex, strain, age, and housing conditions of these rats (Anderson et al., 2014), to verify pellet efficacy and plasma B concentrations relative to intact rats (Fig. 1A). Repeated-measures ANOVA showed main effects for time of day ($F_{1,19} = 7.2$, $P < 0.05$) and interaction between time of day and treatment group ($F_{2,19} = 10.5$, $P < 0.05$). Although B levels held constant throughout the day in ADX + 100B (i.e., 100 mg B) and ADX + 200B (i.e., 200 mg B) groups, sham ADX rats showed lower AM and increased PM plasma B levels (Fig. 1). Pairwise comparisons revealed plasma levels of B in

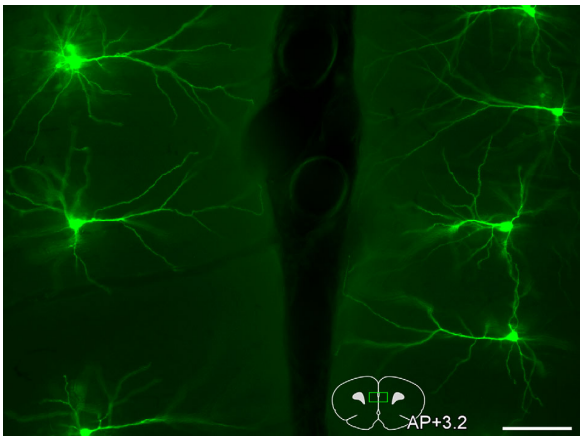

Figure 2. Darkfield photomicrograph depicting an array of bilateral layer 2 and 3 pyramidal neurons in the PL targeted for intracellular dye injection with LY (pseudocolored green). An atlas plate (lower right) depicts the approximate region within the PL in which neurons were filled for morphologic analyses. Distance in millimeters relative to bregma is indicated. AP, anteroposterior. Scale bar = 100 μm.

ADX + 100B and ADX + 200B that were lower in PM and higher in AM, respectively, compared with sham ADX rats ($P < 0.05$ for each; Fig. 1B). These data suggest resultant plasma B levels in the 100B group that roughly approximated the circadian mean (9 μg/dl), with the 200B group displaying closer to circadian peak values (14 μg/dl) compared with sham ADX rats (11 and 16 μg/dl, respectively).

Chronic elevations in plasma B induce dendritic spine loss in PL pyramidal neurons

Figures 2 and 3 illustrate groups of LY-filled pyramidal neurons in layers 2 and 3 of the PL that were subjected to dendritic spine morphometric analyses (198, 106, and 109 dendritic segments in sham, 100B, and 200B groups, respectively). These segments yielded a total of 54,267 dendritic spines subjected to density, subtype, and morphologic analysis (sham, n = 10 rats/27,225 spines; 100B, n = 6 rats/14,458 spines; 200B, n = 6 rats/12,554 spines; Table 1). One-way ANOVA performed at different portions of the dendritic tree revealed most pronounced main effects in distal apical dendrites (i.e., > 150 μm; $F_{2,20} = 3.873$, $P = 0.04$; Fig. 4). ADX + 200B rats displayed a 21% decrease in dendritic spine density within this region and a 13% decrease when combined across all three regions compared with sham ADX rats ($P < 0.01$ for each). By

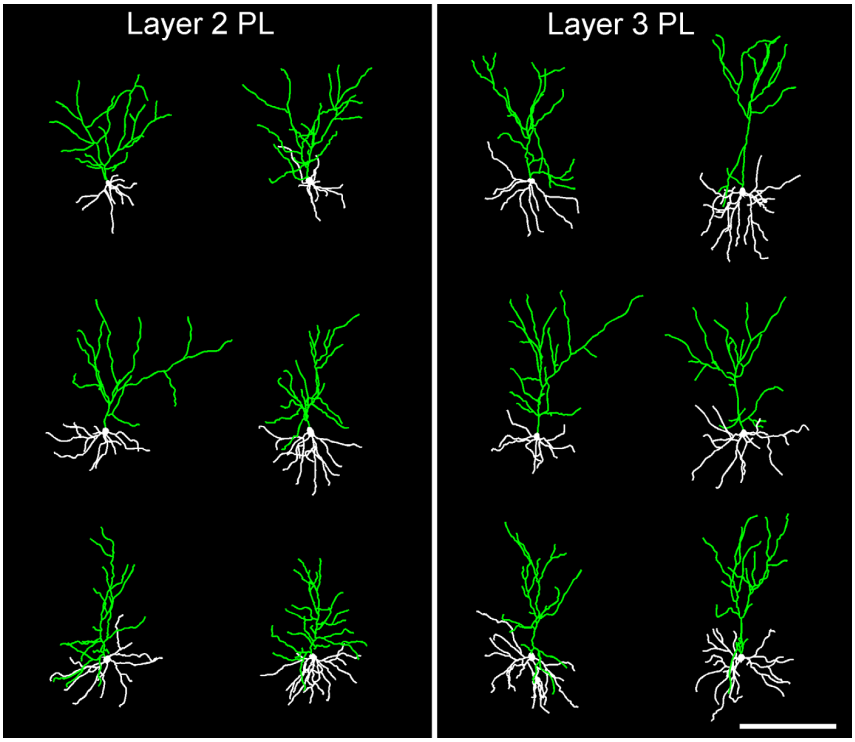

Figure 3. Examples of 3D digital reconstructions showing LY-filled layer 2 (left) and layer 3 (right) pyramidal neurons in the PL. Contrasting apical dendritic morphologies between these neuronal subtypes are highlighted in green, with layer 3 neurons exhibiting apical dendrites with an initial bifurcation point more distal to the cell body than in layer 2. Scale bar = 200 μm.

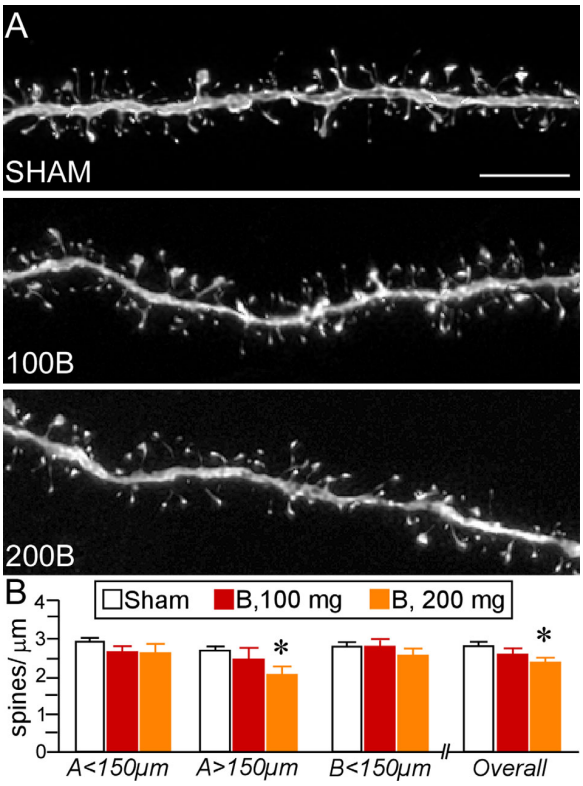

Figure 4. **A**: Deconvolved images of dendritic segments from layer 2 and 3 pyramidal neurons in the PL from different treatment groups. **B**: Mean and SEM of dendritic spine density as a function of B treatment. B100 (i.e., 100 mg B) animals show no differences in spine density relative to controls within any region of the dendritic tree. B200 (i.e., 200 mg B) rats show overall spine loss, notably in the more distal aspects of the apical tree. Control, n = 10; B100 and B200, n = 6. $^{*}P < 0.05$, significantly different from sham rats. Scale bar = 5 µm.

contrast, ADX + 100B treatment failed to produce any reliable differences in dendritic spine density relative to control or 200B-dose groups (Fig. 4, Table 1).

Additional analyses of dendritic arborization patterns (overall length, branch number) in the same set of PL neurons were undertaken to assess the extent to which dendritic spine loss may be accounted for by larger-scale changes in dendritic morphology. These analyses revealed a main effect for apical dendritic length ($F_{2,20} = 3.5$, $P = 0.05$). Post hoc comparisons revealed a 23% reduction in apical dendritic length in B200 rats relative to sham control rats ($P = 0.02$), whereas no significant reduction was evident between 100B and sham control groups ($P = 0.2$; Fig. 5). Prolonged B exposure failed to alter the number of branch endings in apical dendrites and also had no effect on either index in basal dendrites (Fig. 5, Table 1). When apical dendritic shortening and decreases in spine density are taken together, this compounds the net loss of dendritic spines in layers 2 and 3 PL neurons to levels approximating 67% of control values following prolonged high-dose exposure of glucocorticoids.

Effects of high levels of B on PL dendritic spine morphology

Dendritic spines can be distinguished by geometric characteristics (i.e., thin, mushroom, stubby) that have proved to be useful for inferring synaptic structure–function relationships (Kasai et al., 2003; Bourne and Harris, 2007; Yang et al., 2009; Dumitriu et al., 2010; Lee et al., 2012; Fig. 5A). In cortical pyramidal neurons, spines classified as thin represent the majority of the population (60–70%; Bourne and Harris, 2007), and previous studies have identified this subtype as important

TABLE 1.

Data Summary for Experiment 1: Effects of Varying Doses of B on Structural Plasticity in PL

Treatment	Sham	100B	200B
Animals	10	6	6
Neurons	66	36	36
Neurons/animal	6–7	6	6
Laminae analyzed (layers)	2, 3	2, 3	2, 3
Spines	27,225	14,458	12,554
Overall spine density ± SEM	2.75 ± 0.06	2.63 ± 0.17	2.47 ± 0.12[1]
Thin spine density ± SEM	2.13 ± 0.06	2.03 ± 0.15	1.89 ± 0.12[1]
Mushroom spine density ± SEM	0.35 ± 0.02	0.34 ± 0.02	0.33 ± 0.02
Stubby spine density ± SEM	0.27 ± 0.02	0.25 ± 0.01	0.25 ± 0.01
Neurons/animal; dendritic arborization analysis	5, 6[2]	4, 5[2]	4–6[2]
Apical dendrite length	2,819 ± 135	2,467 ± 255	2,164 ± 214[1]
Apical branch endings	15 ± 1.1	14 ± 1.2	14 ± 0.7
Basal dendrite length	617.8 ± 45	568.4 ± 56	519.8 ± 50
Basal branch endings	4.9 ± 0.46	4.5 ± 0.38	4.46 ± 0.38

[1] $P < 0.05$, compared with control treatment group.
[2] Because of strict inclusion criteria (see Materials and Methods), the number of neurons analyzed in the dendritic arborization analysis is smaller than the number of neurons analyzed in the dendritic spine analysis.

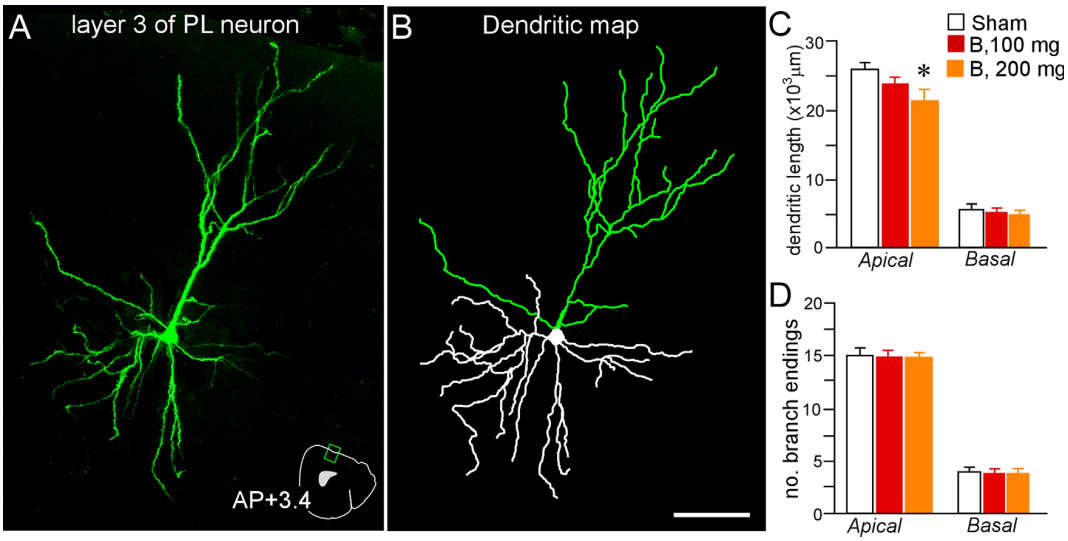

Figure 5. 3D digital reconstruction of LY-filled layer 2 and 3 PL neuron (pseudocolored green) with confocal laser-scanning microscopy (**A**) and the rendering of its dendritic tree with computer-assisted morphometry (**B**). An atlas plate (A, lower right) depicts the neuron's approximate location and angle of orientation within the PL. Distance in millimeters relative to bregma is indicated. AP, anteroposterior. Mean and SEM for dendritic length (**C**) and number of branch endings (**D**) for apical and basal dendrites as a function of treatment group. Only rats that received high-dose glucocorticoids (200 mg) displayed apical dendritic shrinkage. Control, n = 10; B100 and B200 (i.e., 100 and 200 mg B, respectively), n = 6. *$P < 0.05$, significantly different from sham rats. Scale bar = 75 µm.

for long-term potentiation and learning-related plasticity (Arnsten et al., 2010; Anderson et al., 2014). In our analysis of spine subtype (Fig. 6A), thin spines were the most vulnerable to prolonged high-dose glucocorticoid exposure, particularly within more distal apical dendrites ($F_{2,20} = 3.6$, $P < 0.05$). Post hoc comparisons revealed a significant 15% decrement of thin spines in combined apical and basal segments in the 200B group compared with control rats ($P < 0.05$), with the most significant loss on the most distal aspects (by 24%, $P < 0.05$; Fig. 6B). In contrast, examination of thin spine densities in the 100B group failed to demonstrate any reliable shifts relative to control or 200B rats (Fig. 6B, Table 1).

Evaluation of other spine subtypes (mushroom, stubby) did not uncover any differences following prolonged glucocorticoid exposure (Fig. 6C,D). Moreover, additional analyses of several spine parameters (length, head diameter, volume) did not reveal any group differences as a function of glucocorticoid treatment (data not shown). However, population analysis of spine volume revealed cumulative frequency shifts following both regimens of glucocorticoid treatment. Comparison of frequency distributions of overall spine populations revealed downward trends (i.e., leftward shifts) in volume in both 100B and 200B rats relative to control groups ($P = 0.02$ and $P < 0.01$, respectively, K-S test), with the 200B spine population showing an even greater shift relative to 100B ($P < 0.01$, K-S test; Fig. 7A). Examination of frequency shifts in subtypes revealed the greatest effects in thin spines (Fig. 7B); 100B showed a leftward shift relative to controls ($P < 0.01$, K-S test), whereas 200B showed significant shifts relative to both control and 100B populations ($P < 0.01$ for each, K-S test). Cumulative frequencies plotted for mushroom spine subtypes also revealed a leftward shift in the 200B treatment group relative to 100B and control groups ($P < 0.01$ for each, K-S test), whereas the 100B group failed to show any differences in this index relative to the control population ($P = 0.7$, K-S test; Fig. 7C). These observations support the interpretation that prolonged B exposure induces dendritic spine shrinkage in PL neurons even in the absence of any frank loss of spines in the case of low-dose B, whereas high-dose B results in more generalized decreases in spine volume across subtypes as well as attrition of thin spines.

Experiment 2: persistence of B-induced structural alterations in the PL following a 3-week recovery period

Characterization of plasma B levels

Next, we examined whether a washout period following prolonged B exposure would ameliorate the regressive structural alterations in PL dendritic spines (Fig. 8A). In this experiment, we extended our spine morphologic

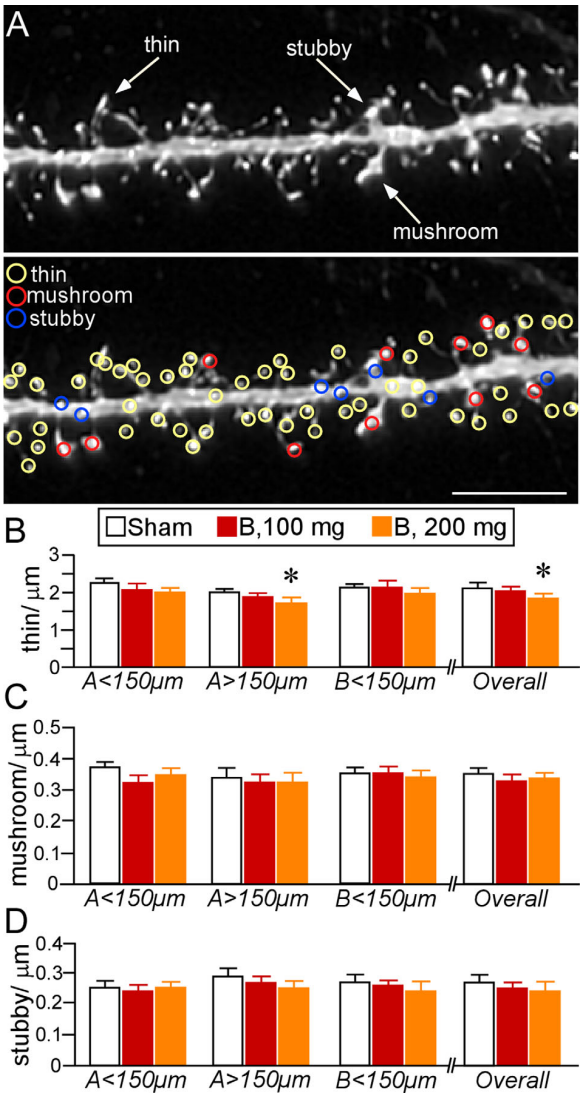

Figure 6. **A**: Example of high-resolution deconvolved optical z-stack of a dendritic segment used for spine analysis in NeuronStudio. Circles designate spine subtypes based on user-defined parameters in the software. **B–D**: Mean ± SEM of dendritic spine subtypes. Thin spine loss was evident in B200 (i.e., 200 mg B) rats (B), especially at radial distances >150 µm. No other effects were evident in other subtypes (C,D). Control, n = 10; B100 and B200, n = 6. *$P < 0.05$, significantly different from sham rats. Scale bar = 5 µm.

analysis to include neurons in layers 2, 3, and 5 to assess the extent to which glucocorticoid-induced spine loss generalizes across different laminae in the PL. On day 14 after steroid implantation, blood samples were collected from the tail vein of rats in the control and 200B + recovery groups to verify pellet efficacy and plasma B concentrations, and blood samples were collected again on day 35 (i.e., in 200B and 200B + recovery groups) to verify the normalization of adrenocortical activity during the washout period. Repeated-measures ANOVA showed main effects for treatment group ($F_{3,45} = 5.3$, $P < 0.05$), time of day ($F_{1,45} = 7.2$, $P < 0.05$), and interaction ($F_{3,45} = 24.0$, $P < 0.05$). B levels remained consistently elevated near the circadian zenith during the 21-day B exposure time frame in both 200B and 200B + recovery groups compared with sham controls (Fig. 8B). 200B + recovery rats displayed normalization of AM and PM levels of plasma B when assayed during the washout period on day 35 (Fig. 8B).

Lack of normalization in PL dendritic spine morphology following recovery from B exposure

In this experiment, 460 dendritic segments from 153 fluorescent dye-labeled PL neurons in layers 2, 3, and 5 were analyzed for spine density and morphometric analysis (120, 160, and 180 dendritic segments in control, 200B, and 200B + recovery groups, respectively). These segments yielded a total of 61,600 dendritic spines subjected to density, subtype, and morphologic analysis (sham, n = 6 rats/17,400 spines; 200B, n = 7 rats/20,800 spines; 200B + recovery, n = 8 rats/23,400 spines; Table 2). One-way ANOVA of spine density in layers 2, 3, and 5 pyramidal neurons revealed a main effect as a function of experimental treatment ($F_{2,18} = 4.6$, $P < 0.05$; Fig. 9A–C). Post hoc analyses revealed significant decreases in 200B and 200B + recovery groups relative to controls (by 16%, $P < 0.05$ for each; Fig. 9C), suggesting that a 21-day washout period was insufficient to reverse glucocorticoid-induced decrements in spine density, even after normalization of circadian adrenocortical activity. Regional analysis of apical and basal subdivisions demonstrated downward trends throughout, with statistically significant reductions evident in the proximal region of the apical tree in the 200B group ($P < 0.05$) and basal dendrites of the 200B + recovery group ($P < 0.05$) relative to controls. In contrast, no trends or statistically significant differences in spine density were evident in the 200B and 200B + recovery groups.

Examination of spine subtype revealed generalized downward trends in both 200B and 200B + recovery groups. These effects were most noteworthy in overall mushroom ($F_{2,18} = 3.5$, $P = 0.052$) and overall thin ($F_{2,18} = 2.8$, $P = 0.08$) categories; however, neither was statistically significant (Fig. 9D–F). Followup analysis of population shifts in spine volume revealed significant decrements in both 200B and 200B + recovery groups compared with control animals ($P < 0.01$ for each, K-S test), whereas the frequency distributions between

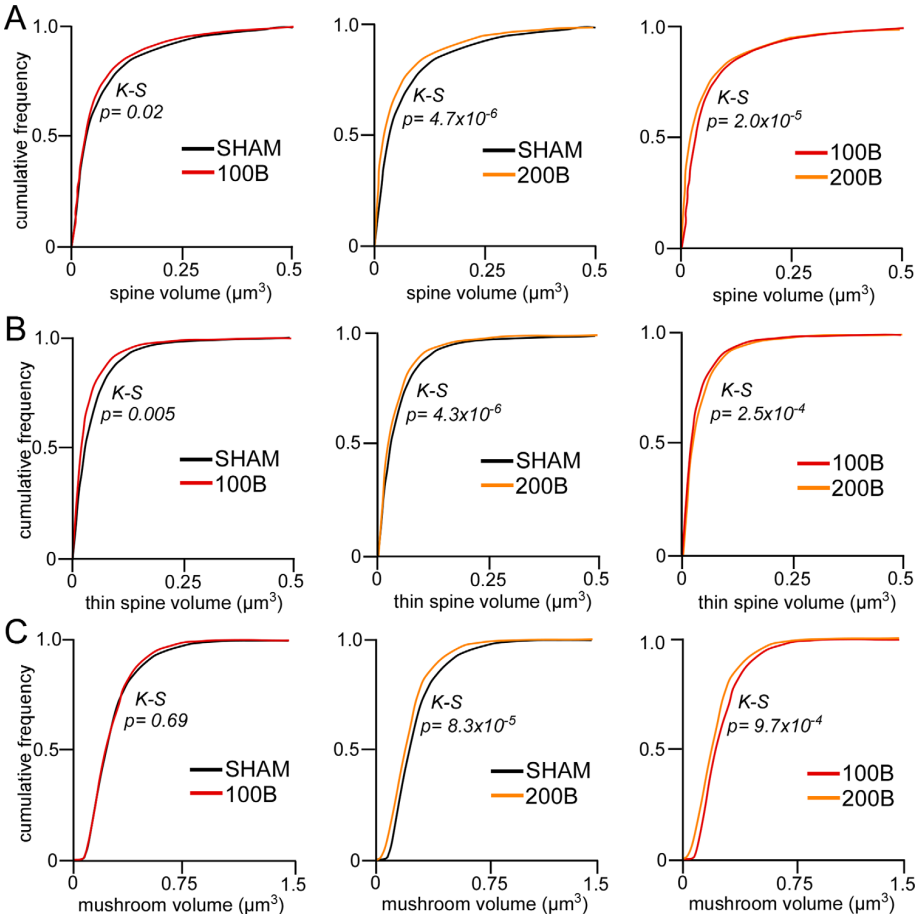

Figure 7. **A**: Cumulative frequency distributions of overall spine volume in PL neurons reveal graded leftward shifts (i.e., decrease) in spine volume in 100B and 200B (i.e., 100 and 200 mg B, respectively) rats. **B**: This trend is recapitulated in thin spine volumes. **C**: In contrast, B200 rats show selective decreases in mushroom spine volumes relative to B100 and sham groups. Significance set at $P < 0.01$, K-S test.

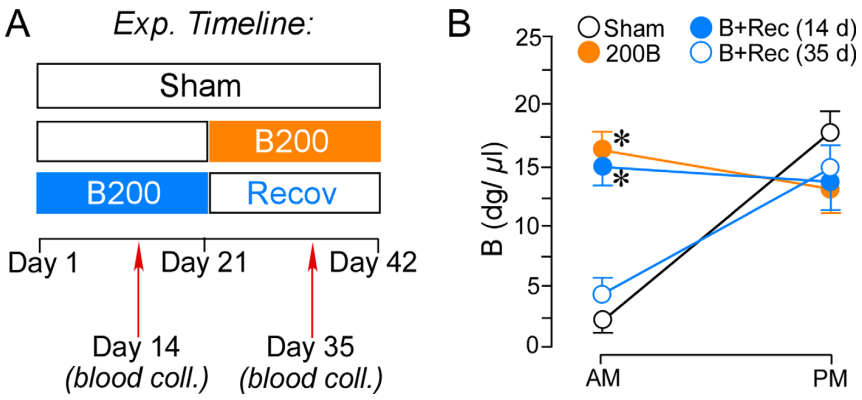

Figure 8. **A**: Time line of the second experiment for high-dose B treatment (B200) and comparison with groups of rats given a 3-week recovery period (B + Recov) to restore HPA rhythmicity. On day 14, blood was collected in sham and B + Recov animals to assay for effectiveness of pellet increasing B levels. On day 35, blood was collected to assay for effectiveness of pellet increasing B levels in B200 animals and in B + Recov to assay for HPA activity restoration. **B**: B200 and B200 + Recov (Rec) groups show elevated B, and B + Rec rats show a normalization of adrenocortical function after the cessation of B exposure. N = 6–8 rats/group. $^*P < 0.05$, significantly different from sham group.

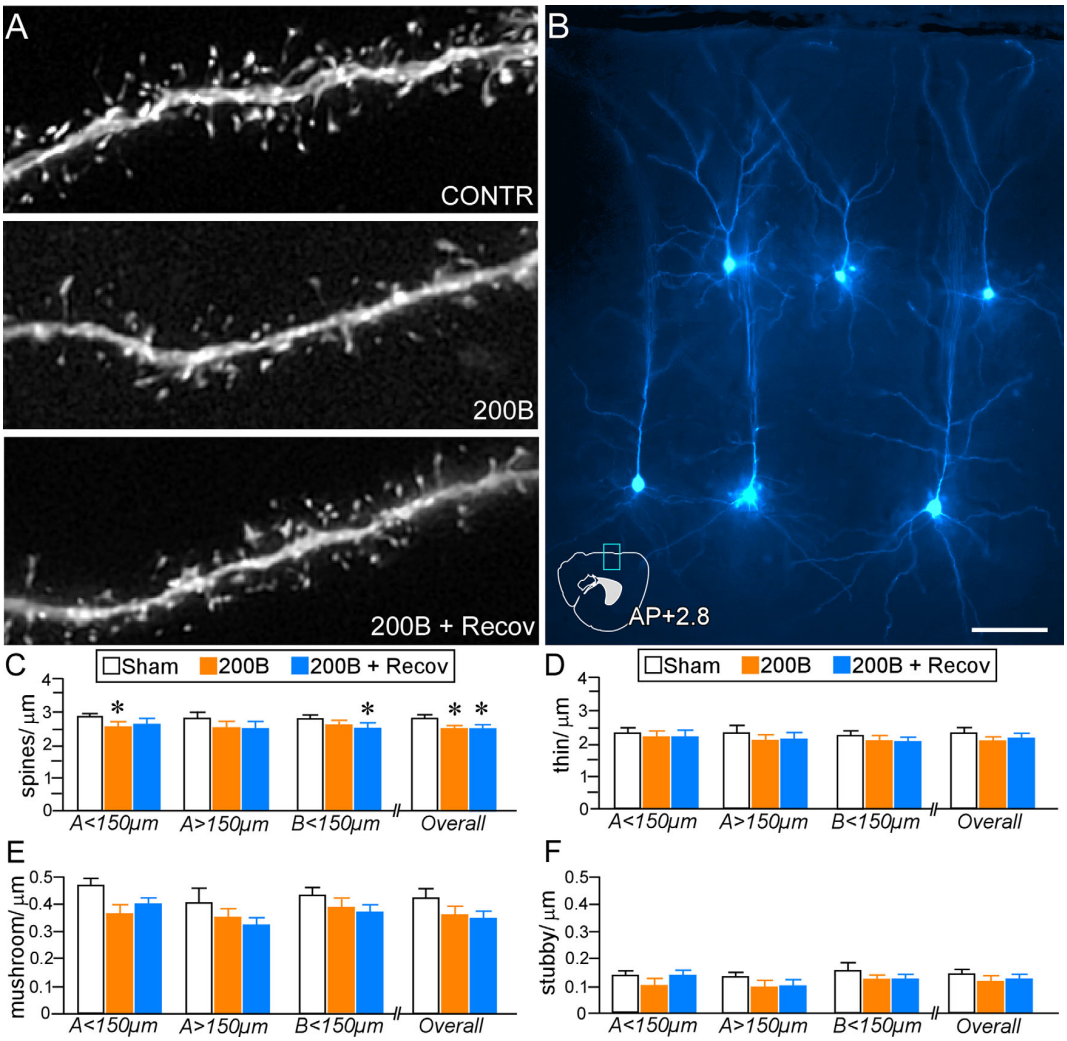

Figure 9. **A**: Deconvolved images of dendritic segments from pyramidal neurons in the PL from different treatment groups. **B**: Image depicts several layer 2, 3, and 5 dye-filled PL pyramidal neurons (pseudocolored cyan). An atlas plate (lower left) depicts the approximate location and orientation within the PL of the dye-filled neurons as shown. Distance in millimeters relative to bregma is indicated. AP, anteroposterior. Mean and SEM of dendritic spine density (**C**) and thin subtype density (**D**) as a function of experimental treatment. Both 200B and B200 + recovery (Recov) groups show overall decreases in density relative to sham rats, whereas only 200B rats show significant reductions in overall thin subtypes. Mean and SEM of mushroom (**E**) and stubby (**F**) spine densities in treatment groups. Both 200B and 200B + Recov groups display evidence of mushroom spine loss at various regions of the dendritic tree, whereas 200B + Recov rats show overall decreases, relative to sham control rats. N = 6–8 rats per group $^*P < 0.05$, significantly different relative to sham group. Scale bar = 5 µm.

200B and 200B + recovery groups were not statistically different ($P = 0.11$, K-S test; Fig. 10A). Population analyses performed within thin and mushroom spines also revealed similar leftward (downward) shifts in volume in 200B and 200B + recovery groups relative to controls ($P < 0.01$ for each, K-S test), whereas no statistically significant differences were noted via comparison of cumulative distributions between 200B and 200B + recovery groups (Fig. 10B,C). These data endorse the results from the first experiment that high-dose glucocorticoid exposure may induce a persistent attrition of dendritic spines throughout pyramidal neurons in the PL, likely via one or multiple mechanisms involving spine pruning and shrinkage.

Experiment 3: effects of short-term B exposure on structural plasticity in the PL

Because the first two experiments had demonstrated that 2 weeks or longer of prolonged high-dose glucocorticoid exposure induces regressive structural plasticity

TABLE 2.

Data Summary for Experiment 2: Persistence of B-Induced Structural Alterations in PL Following a 3-Week Recovery Period

Treatment	Sham	200B	200B + recovery
Animals	6	7	8
Neurons	40	53	60
Neurons/animal	6, 7	7, 8	7, 8
Laminae analyzed (layers)	2, 3, 5	2, 3, 5	2, 3, 5
Spines	17,400	20,800	23,400
Overall spine density ± SEM	2.87 ± 0.07	2.62 ± 0.08[1]	2.61 ± 0.08[1]
Thin spine density ± SEM	2.31 ± 0.07	2.12 ± 0.07	2.11 ± 0.07
Mushroom spine density ± SEM	0.43 ± 0.01	0.4 ± 0.02	0.38 ± 0.02
Stubby spine density ± SEM	0.13 ± 0.01	0.11 ± 0.01	0.12 ± 0.01
Neurons/animal; dendritic arborization analysis	N/A	N/A	N/A
Apical dendrite length	N/A	N/A	N/A
Apical branch endings	N/A	N/A	N/A
Basal dendrite length	N/A	N/A	N/A
Basal branch endings	N/A	N/A	N/A

[1] $P < 0.05$ compared with control treatment group.

in PL neurons, in a final experiment we addressed whether a shorter duration (i.e., 1 week) of high-dose B exposure could produce similar changes. In these studies, we again restricted our analyses to PL neurons within layers 2 and 3 to compare both dendritic morphology and spine density. Nevertheless, this analysis

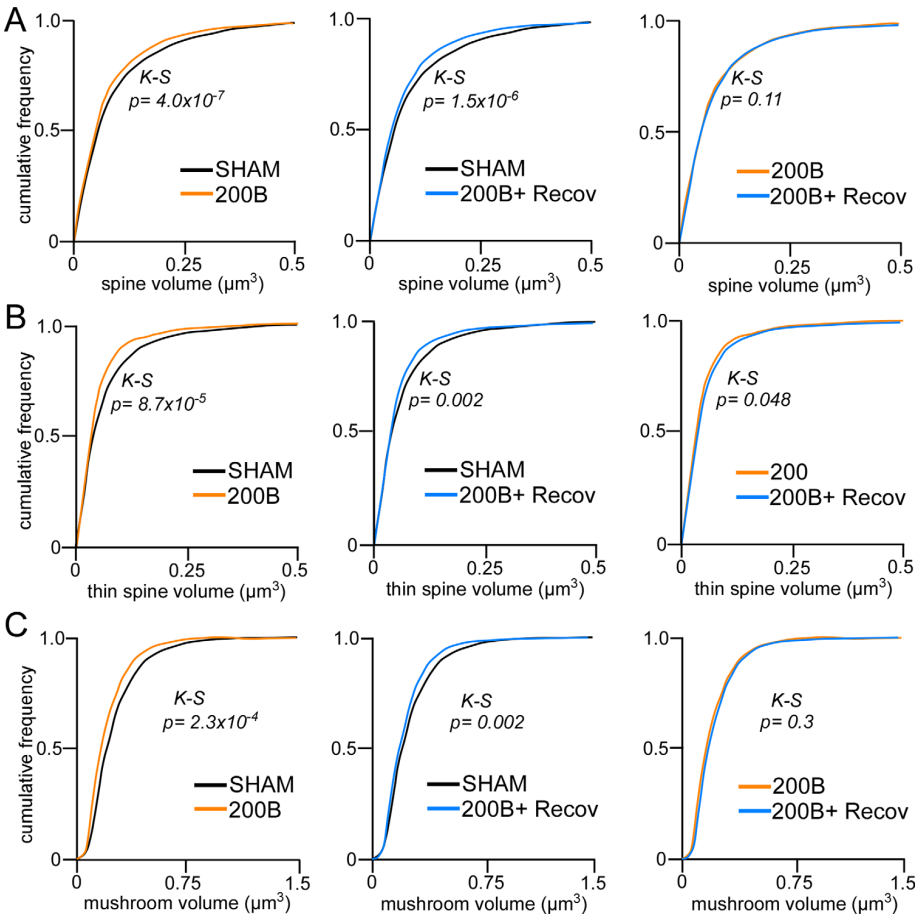

Figure 10. **A**: Cumulative frequency distributions of overall spine volume in PL neurons reveal leftward shifts (i.e., decrease) in spine volume following 200B treatment, even after a 21-day recovery period. This trend is also evident in thin (**B**) and mushroom (**C**) subtypes with respect to sham control rats. Significance set at $P < 0.01$, K-S test.

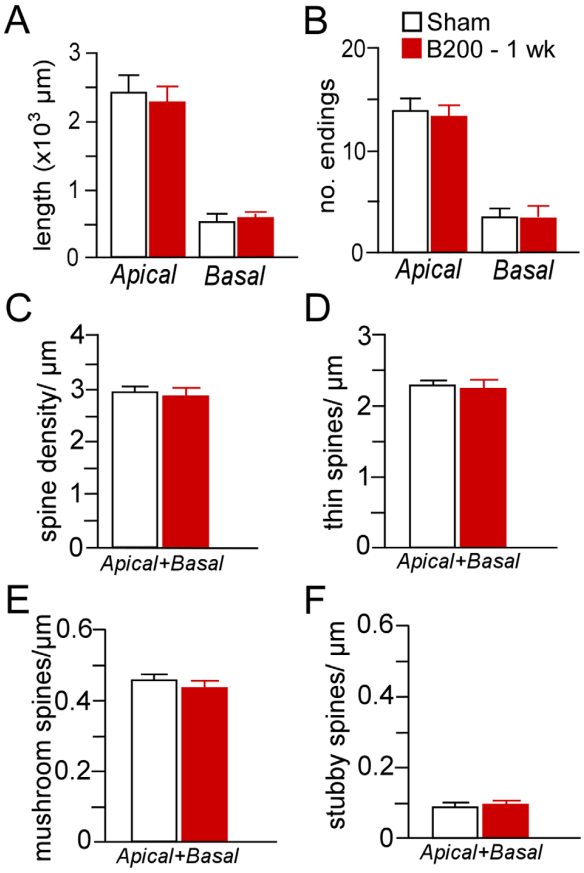

Figure 11. Mean and SEM for dendritic length (**A**) and number of branch endings (**B**) after 1 week of exposure to high-dose B (200-mg pellet, s.c.). Mean and SEM for overall (**C**), thin (**D**), mushroom (**E**), and stubby (**F**) spine densities as a function of B200 or sham pellets. This duration of glucocorticoid exposure failed to induce any frank differences in the dendritic or spine morphologic indices examined in PL neurons. N = 5–6 rats per group.

failed to reveal any effects on any of the structural indices examined (Fig. 11, Table 3). These data, when taken together with the other two experiments, suggest that >1 week of continuous exposure to glucocorticoids is required for the induction of regressive modifications in PL neurons.

DISCUSSION

It has been widely documented that chronic stress leads to the reorganization of neuronal architecture in the mPFC. Here, we expand on these findings by showing that increasing plasma levels of B over a period of at least 2 weeks induces apical dendritic shortening, spine loss, and morphological alterations in PL pyramidal neurons. A more surprising result is that these structural alterations persist even after a washout period and its attendant restoration of circadian B secretory activity. These data generally endorse the view that chronic stress-induced effects on prefrontal structural plasticity involve a glucocorticoid-dependent component. However, they contrast with the effects of repeated stress, whereby recovery periods restore dendrite and spine morphologic indices (Radley et al., 2005; Bloss et al., 2010, 2011). It is worth emphasizing that prolonged elevations in glucocorticoids are not taken to be equivalent to stress. In fact, elevated glucocorticoids may be more broadly representative of dysregulated homeostatic parameters produced by systemic diseases or by prolonged pharmacotherapeutic regimens under certain chronic conditions. Therefore, our data implicate disrupted adrenocortical function in the induction of protracted synaptic reorganization in the mPFC that may follow prolonged stress or other diseases involving endocrine disruptions.

Methodological considerations

Many repeated stress manipulations are known to decrease dendrite and spine morphologic indices reliably throughout mPFC subfields in the rat (Cook and Wellman, 2004; Radley et al., 2004, 2008; Liston et al., 2006; Michelsen et al., 2007; Perez-Cruz et al., 2007; Liu and Aghajanian, 2008; Dias-Ferreira et al., 2009; Hains et al., 2009; Holmes and Wellman, 2009; Shansky et al., 2009). However, previous work investigating the effects of repeated B exposure on mPFC structural plasticity has produced mixed results. In one series of studies, repeated daily glucocorticoid injections for 3 weeks differentially altered mPFC pyramidal neuron dendritic morphology, marked by increased and decreased dendritic branching patterns in proximal and distal aspects of the dendritic tree, respectively, and increased dendritic spine density in the same cell types (Wellman, 2001; Seib and Wellman, 2003). Another study showed decreased dendrite length, branching patterns, and anatomical regional volumes in mPFC subfields, with no change in spine density after 1 month of daily glucocorticoid injections (Cerqueira et al., 2005, 2007). In contrast, studies that have administered corticosteroids through drinking water for 10–20 days have also observed mPFC spine density decrements comparable to those induced by stress (Liu and Aghajanian, 2008; Gourley et al., 2013). Although it is possible that some of these discrepancies are attributable to varying modes of glucocorticoid administration (i.e., injections, drinking water, subcutaneous implants), different approaches for visualization and quantification of spines are also likely contributors. For instance, much of the information from this field of study is derived from the Golgi impregnation method, yet recent evidence suggests that this approach undersamples dendritic spine

TABLE 3.
Data Summary for Experiment 3: Effects of Short-Term B Exposure on Structural Plasticity in PL

Treatment	Sham	200B 1 week
Animals	6	5
Neurons	34	26
Neurons/animal	5, 6	5, 6
Laminae analyzed (layers)	2, 3	2, 3
Spines	13,095	10,763
Overall spine density ± SEM	2.91 ± 0.13	2.87 ± 0.10
Thin spine density ± SEM	2.37 ± 0.11	2.35 ± 0.07
Mushroom spine density ± SEM	0.45 ± 0.02	0.42 ± 0.03
Stubby spine density ± SEM	0.09 ± 0.01	0.10 ± 0.01
Neurons/animal; dendritic arborization analysis	4, 5[1]	4, 5[1]
Apical dendrite length	1,814 ± 261	1,679 ± 167
Apical branch endings	12 ± 1.5	11 ± 1.1
Basal dendrite length	329 ± 38	340 ± 30
Basal branch endings	2.8 ± 0.22	2.9 ± 0.17

[1]Because of strict inclusion criteria (see Materials and Methods), the number of neurons analyzed in the dendritic arborization analysis is smaller than the number of neurons analyzed in the dendritic spine analysis.

densities (by > 50%) and specifically biases against the identification of thin subtypes (for a discussion of this issue see Dumitriu et al., 2011, 2012; Radley et al., 2015). Nevertheless, the present results and the weight of prior evidence support our interpretation that prolonged glucocorticoid exposure leads to regressive and persistent dendritic spine alterations in mPFC neurons.

The current study also highlights the importance of applying more refined technical approaches to understand glucocorticoid effects on structural plasticity better. In another line of investigation, Liston and Gan (2011) applied two-photon microscopy for time-lapse imaging of dendritic spines in the mouse somatosensory cortex (S1) and showed that prolonged glucocorticoid exposure concurrently eliminated existing spines and prevented new spine formation. Although there are some constraints in the level of resolution that is currently achievable with in vivo two-photon microscopy, the ability to perform repeated sampling has provided fundamentally important information with respect to how glucocorticoids influence spine dynamics (Liston et al., 2013). Electron microscopic approaches will continue to provide important ultrastructural detail for understanding glucocorticoid effects on synaptic alterations, and emerging developments in automated technologies may soon allow higher throughput screening at this level of resolution (see, e.g., Kasthuri et al., 2015). In the meantime, the dendritic spine morphometric approach employed here balances the attainment of high-quality resolution with high-throughput that cannot yet be achieved with other methods.

Interpretive considerations

Comparing and contrasting data from each of the experiments presented in this report raises some interesting questions with respect to possible differences in effects of glucocorticoids on dendritic spine alterations. First, we failed to observe consistent decreases in thin spine subtypes as a function of glucocorticoids across experiments. In the initial experiment, high-dose treatment with B for 2 weeks induced significant decrements in spine density that were manifested by a clear loss of thin spines in PL neurons, whereas, in the second experiment, 3-week B exposure failed to result in a statistically significant reduction in this subtype (e.g., Fig. 9D). This likely is due to the fact that the former experiment examined only layer 3 PL neurons, and the latter involved the analysis of both layer 3 and layer 5 PL neurons. Because we often observe lower overall spine densities in layer 5 relative to layer 3 pyramidal neurons in the mPFC (Anderson and Radley, unpublished observations), combining these into one analysis might have increased the variance enough to reduce the reliability of the observed effects. Given that experience-dependent dendritic spine plasticity has been shown to vary as a function of apical dendritic morphology in layer 5 neurons in S1 (Holtmaat et al., 2006), it is possible that our failure to examine dendritic morphology in layer 5 PL neurons or partition subpopulations accordingly added an additional source of variability in experiment 2.

A second interpretive issue concerns whether rats that were subjected to a longer period of B exposure (i.e., 3 weeks in the second experiment as opposed to 2 weeks in the first) might have shown greater spine loss in the PL. Although there were no frank differences in the overall proportion of spines lost between experiments (by 13% and 16% in experiments 1 and 2, respectively), the second experiment revealed more expansive downward trends in both thin ($P = 0.08$) and mushroom ($P = 0.052$) subtypes, whereas the first displayed only decreases in thin and no downward trend in mushroom subtypes. Because mushroom spines are representative of a category of larger volume, stable, and mature synaptic phenotypes (Harris and Stevens, 1989; Kasai et al., 2003; Holtmaat et al., 2005; Knott et al., 2006; Yasumatsu et al., 2008), one possibility is that B-induced spine shrinkage of this subtype requires longer intervals of steroid exposure. In this scenario, mushroom spine shrinkage could fall below our threshold criteria for being classified as mushroom (i.e., spine head diameter > 0.4 μm; see Materials and Methods), resulting in their reclassification as thin. The idea that an extended period of glucocorticoid exposure can lead

to the selective targeting of large-volume spines is supported by at least two studies (Tanokashira et al., 2012; Liston et al., 2013) and may involve rearrangement of the F-actin network in the spine head via downregulation of the stabilizing protein caldesmon (Tanokashira et al., 2012). This caldesmon-dependent signaling pathway underlying spine shrinkage is also distinct from the aforementioned mechanisms for spine formation/elimination, raising the possibility that the spine loss and shrinkage that we observed following high-dose B treatment may be regulated via distinct mechanisms. Support for this idea might also derive from the observation that prolonged lower dose B treatment in the first experiment resulted in reliable decreases only in spine volume.

Our results in the second experiment show that, after 3 weeks of repeated B exposure, dendritic spine alterations were evident even in rats provided with a 3-week washout period that allowed for the normalization of HPA rhythmicity after high-dose B exposure. At least one previous study has shown that dendritic spine decreases in prefrontal subfields exhibit regionally differentiated patterns of partial recovery following prolonged B exposure (i.e., in infralimbic but not orbitofrontal cortex) after a 7-day washout period (Gourley et al., 2013). One possibility is that the PL may be less resilient to corticosteroid-induced dendritic spine alterations, even the restoration of HPA rhythmicity, although more work is required to understand better how stressful or traumatic experiences may induce long-lasting disruptions in prefrontal networks.

The data presented here may also help to conceptualize how hypercortisolism in Cushing's syndrome or aging could lead to enduring regressive structural and functional changes in mPFC synaptic networks. Patients with Cushing's syndrome display cognitive and prefrontal functional deficits that linger after the normalization of glucocorticoids (Tiemensma et al., 2010a,b; for review see Andela et al., 2015). Recent evidence suggests that diminished prefrontal functional connectivity and cortical thinning in Cushing's syndrome persist even after long-term remission of elevated glucocorticoids (Crespo et al., 2014; Bas-Hoogendam et al., 2015). The cumulative exposure to glucocorticoids in rats has also recently been implicated in age-related decreases in dendritic spine density in mPFC and prefrontal functioning (Anderson et al., 2014), although many studies have linked elevated glucocorticoids in aging with hippocampal and prefrontal impairments (see, e.g., Landfield, 1978; Issa et al., 1990; Sapolsky, 1992; Lupien et al., 1994; Mizoguchi et al., 2009; Franz et al., 2011; Garrido et al., 2012).

Role of disruptions in the adrenocortical rhythm

One lingering question concerns the extent to which B-mediated prefrontal structural alterations may be explained by elevated plasma levels, per se, or the resultant disruption of circadian rhythmicity resulting from the continuous release of steroid into the circulation achieved with subcutaneous implants. Because HPA axis dysregulation may often reflect a flattening of the B secretory rhythm in a variety of human clinical disorders (see, e.g., Miller et al., 2007; Hall et al., 2015), this may have relevance for the repeated glucocorticoid regimen used in the present study. Studies utilizing other methods of repeated B administration that likely enhance circadian peaks of B have also observed similar effects on structural plasticity (Liu and Aghajanian, 2008; Liston and Gan, 2011; Gourley et al., 2013; Swanson et al., 2013), although information is not yet forthcoming regarding the precise morphological differences in spine volume and subtype under these varying regimens of glucocorticoid treatment. Several recent studies have linked glucocorticoid circadian rhythmicity to natural variations in spine formation and elimination (i.e., in somatosensory cortex and hippocampus; Liston et al., 2013; Ikeda et al., 2015). In two other studies, disruption of the circadian photoperiod induced regressive structural changes in the hippocampus and the mPFC along with corresponding cognitive impairments (Pyter et al., 2005; Karatsoreos et al., 2011). These latter studies warrant consideration with respect to whether changes in adrenocortical secretory patterns underlie cognitive impairments following circadian disruption and the extent to which changes in circadian secretory patterns vs. increased levels of B account for prefrontal structural and functional alterations in other experimental and clinical contexts.

Functional considerations

Thin spine subtypes in prefrontal neurons have proved to be highly vulnerable to pruning in response to a variety of contexts, including aging and chronic stress (Dumitriu et al., 2010; Bloss et al., 2011; Radley et al., 2013; Anderson et al., 2014). More recently, thin spine loss in the prefrontal cortex has been implicated in psychiatric illnesses, such as schizophrenia, and psychostimulant use (Arnsten et al., 2010; McEwen and Morrison, 2013; Radley et al., 2015), and our data implicate altered adrenocortical functioning as a contributing factor to prefrontal synaptic reorganization in these settings. One important question concerns whether prolonged glucocorticoid exposure decreases thin spines through a mechanism involving impaired

spine formation and/or increased elimination. Recent evidence suggests that short-term exposure to glucocorticoids mediates both processes via separate signaling pathways, spine formation via glucocorticoid receptor (GR) type I activation via an LIM kinase-cofilin pathway and spine elimination through a GR type II transcriptionally dependent mechanism (Liston et al., 2013). Future studies are required to understand better the precise mechanisms underlying prefrontal spine attrition in response to prolonged periods of glucocorticoid exposure, chronic stress, and other contexts involving altered adrenocortical functioning.

CONFLICT OF INTEREST STATEMENT

The authors declare no competing financial interests.

ROLE OF AUTHORS

RMA and JJR designed research. RMA, RMG, SBJ, MMM, SR-M, and JJR performed research. RMA, RMG, and JJR analyzed data. RMA and JJR wrote the article.

LITERATURE CITED

Alfarez DN, De Simoni A, Velzing EH, Bracey E, Joels M, Edwards FA, Krugers HJ. 2009. Corticosterone reduces dendritic complexity in developing hippocampal CA1 neurons. Hippocampus 19:828–836.

Andela CD, van Haalen FM, Ragnarsson O, Papakokkinou E, Johannsson G, Santos A, Webb SM, Biermasz NR, van der Wee NJ, Pereira AM. 2015. Mechanisms in endocrinology: Cushing's syndrome causes irreversible effects on the human brain: a systematic review of structural and functional magnetic resonance imaging studies. Eur J Endocrinol 173:R1–R14.

Anderson RM, Birnie AK, Koblesky NK, Romig-Martin SA, Radley JJ. 2014. Adrenocortical status predicts the degree of age-related deficits in prefrontal structural plasticity and working memory. J Neurosci 34:8387–8397.

Antoni FA. 1986. Hypothalamic control of adrenocorticotropin secretion: advances since the discovery of 41-residue corticotropin-releasing factor. Endocr Rev 7:351–378.

Arnsten AF, Paspalas CD, Gamo NJ, Yang Y, Wang M. 2010. Dynamic network connectivity: a new form of neuroplasticity. Trends Cogn Sci 14:365–375.

Bas-Hoogendam JM, Andela CD, van der Werff SJ, Pannekoek JN, van Steenbergen H, Meijer OC, van Buchem MA, Rombouts SA, van der Mast RC, Biermasz NR, van der Wee NJ, Pereira AM. 2015. Altered neural processing of emotional faces in remitted Cushing's disease. Psychoneuroendocrinology 59:134–146.

Bloss EB, Janssen WG, McEwen BS, Morrison JH. 2010. Interactive effects of stress and aging on structural plasticity in the prefrontal cortex. J Neurosci 30:6726–6731.

Bloss EB, Janssen WG, Ohm DT, Yuk FJ, Wadsworth S, Saardi KM, McEwen BS, Morrison JH. 2011. Evidence for reduced experience-dependent dendritic spine plasticity in the aging prefrontal cortex. J Neurosci 31:7831–7839.

Bourne J, Harris KM. 2007. Do thin spines learn to be mushroom spines that remember? Curr Opin Neurobiol 17: 381–386.

Cerqueira JJ, Pego JM, Taipa R, Bessa JM, Almeida OF, Sousa N. 2005. Morphological correlates of corticosteroid-induced changes in prefrontal cortex-dependent behaviors. J Neurosci 25:7792–7800.

Cerqueira JJ, Taipa R, Uylings HB, Almeida OF, Sousa N. 2007. Specific configuration of dendritic degeneration in pyramidal neurons of the medial prefrontal cortex induced by differing corticosteroid regimens. Cereb Cortex 17:1998–2006.

Cook SC, Wellman CL. 2004. Chronic stress alters dendritic morphology in rat medial prefrontal cortex. J Neurobiol 60:236–248.

Crespo I, Esther GM, Santos A, Valassi E, Yolanda VG, De Juan-Delago M, Webb SM, Gomez-Anson B, Resmini E. 2014. Impaired decision-making and selective cortical frontal thinning in Cushing's syndrome. Clin Endocrinol 81:826–833.

Dias-Ferreira E, Sousa JC, Melo I, Morgado P, Mesquita AR, Cerqueira JJ, Costa RM, Sousa N. 2009. Chronic stress causes frontostriatal reorganization and affects decision making. Science 325:621–625.

Diorio D, Viau V, Meaney MJ. 1993. The role of the medial prefrontal cortex (cingulate gyrus) in the regulation of hypothalamic–pituitary–adrenal responses to stress. J Neurosci 13:3839–3847.

Dumitriu D, Hao J, Hara Y, Kaufmann J, Janssen WG, Lou W, Rapp PR, Morrison JH. 2010. Selective changes in thin spine density and morphology in monkey prefrontal cortex correlate with aging-related cognitive impairment. J Neurosci 30:7507–7515.

Dumitriu D, Rodriguez A, Morrison JH. 2011. High-throughput, detailed, cell-specific neuroanatomy of dendritic spines using microinjection and confocal microscopy. Nat Protoc 6:1391–1411.

Dumitriu D, Laplant Q, Grossman YS, Dias C, Janssen WG, Russo SJ, Morrison JH, Nestler EJ. 2012. Subregional, dendritic compartment, and spine subtype specificity in cocaine regulation of dendritic spines in the nucleus accumbens. J Neurosci 32:6957–6966.

Feldman S, Conforti N. 1980. Participation of the dorsal hippocampus in the glucocorticoid feedback effect on adrenocortical activity. Neuroendocrinology 30:52–55.

Franz CE, O'Brien RC, Hauger RL, Mendoza SP, Panizzon MS, Prom-Wormley E, Eaves LJ, Jacobson K, Lyons MJ, Lupien S, Hellhammer D, Xian H, Kremen WS. 2011. Cross-sectional and 35-year longitudinal assessment of salivary cortisol and cognitive functioning: the Vietnam era twin study of aging. Psychoneuroendocrinology 36:1040–1052.

Gabbott PL, Warner TA, Jays PR, Salway P, Busby SJ. 2005. Prefrontal cortex in the rat: projections to subcortical autonomic, motor, and limbic centers. J Comp Neurol 492:145–177.

Garrido P, De Blas M, Gine E, Santos A, Mora F. 2012. Aging impairs the control of prefrontal cortex on the release of corticosterone in response to stress and on memory consolidation. Neurobiol Aging 33:827 e1–e9.

Gourley SL, Swanson AM, Koleske AJ. 2013. Corticosteroid-induced neural remodeling predicts behavioral vulnerability and resilience. J Neurosci 33:3107–3112.

Grillo CA, Risher M, Macht VA, Bumgardner AL, Hang A, Gabriel C, Mocaer E, Piroli GG, Fadel JR, Reagan LP. 2015. Repeated restraint stress-induced atrophy of glutamatergic pyramidal neurons and decreases in glutamatergic efflux in the rat amygdala are prevented by the antidepressant agomelatine. Neuroscience 284:430–443.

Hains AB, Vu MA, Maciejewski PK, van Dyck CH, Gottron M, Arnsten AF. 2009. Inhibition of protein kinase C signaling

protects prefrontal cortex dendritic spines and cognition from the effects of chronic stress. Proc Natl Acad Sci U S A 106:17957–17962.

Hall BS, Moda RN, Liston C. 2015. Glucocorticoid mechanisms of functional connectivity changes in stress-related neuropsychiatric disorders. Neurobiol Stress 1:174–183.

Harris KM, Stevens JK. 1989. Dendritic spines of CA 1 pyramidal cells in the rat hippocampus: serial electron microscopy with reference to their biophysical characteristics. J Neurosci 9:2982–2997.

Herman JP, Cullinan WE, Morano MI, Akil H, Watson SJ. 1995. Contribution of the ventral subiculum to inhibitory regulation of the hypothalamo–pituitary–adrenocortical axis. J Neuroendocrinol 7:475–482.

Hinwood M, Morandini J, Day TA, Walker FR. 2012. Evidence that microglia mediate the neurobiological effects of chronic psychological stress on the medial prefrontal cortex. Cereb Cortex 22:1442–1454.

Holmes A, Wellman CL. 2009. Stress-induced prefrontal reorganization and executive dysfunction in rodents. Neurosci Biobehav Rev 33:773–783.

Holtmaat AJ, Trachtenberg JT, Wilbrecht L, Shepherd GM, Zhang X, Knott GW, Svoboda K. 2005. Transient and persistent dendritic spines in the neocortex in vivo. Neuron 45:279–291.

Ikeda M, Hojo Y, Komatsuzaki Y, Okamoto M, Kato A, Takeda T, Kawato S. 2015. Hippocampal spine changes across the sleep-wake cycle: corticosterone and kinases. J Endocrinol 226:M13-M27.

Issa AM, Rowe W, Gauthier S, Meany MJ. 1990. Hypothalamic–pituitary–adrenal activity in aged, cognitively impaired, and cognitively unimpaired rats. J Neurosci 10:3247–3254.

Jaferi A, Bhatnagar S. 2006. Corticosterone can act at the posterior paraventricular thalamus to inhibit hypothalamic–pituitary–adrenal activity in animals that habituate to repeated stress. Endocrinology 147:4917–4930.

Karatsoreos IN, Bhagat S, Bloss EB, Morrison JH, McEwen BS. 2011. Disruption of circadian clocks has ramifications for metabolism, brain, and behavior. Proc Natl Acad Sci U S A 108:1657–1662.

Kasai H, Matsuzaki M, Noguchi J, Yasumatsu N, Nakahara H. 2003. Structure–stability–function relationships of dendritic spines. Trends Neurosci 26:360–368.

Kasper EM, Larkman AU, Lubke J, Blakemore C. 1994. Pyramidal neurons in layer 5 of the rat visual cortex. I. Correlation among cell morphology, intrinsic electrophysiological properties, and axon targets. J Comp Neurol 339:459–474.

Kasthuri N, Hayworth KJ, Berger DR, Schalek RL, Conchello JA, Knowles-Barley S, Lee D, Vazquez-Reina A, Kaynig V, Jones TR, Roberts M, Morgan JL, Tapia JC, Seung HS, Roncal WG, Vogelstein JT, Burns R, Sussman DL, Priebe CE, Pfister H, Lichtman JW. 2015. Saturated reconstruction of a volume of neocortex. Cell 162:648–661.

Knott GW, Holtmaat A, Wilbrecht L, Welker E, Svoboda K. 2006. Spine growth precedes synapse formation in the adult neocortex in vivo. Nat Neurosci 9:1117–1124.

Krettek JE, Price JL. 1977. Projections from the amygdaloid complex to the cerebral cortex and thalamus in the rat and cat. J Comp Neurol 172:687–722.

Landfield PW. 1978. An endocrine hypothesis of brain aging and studies on brain–endocrine correlations and monosynaptic neurophysiology during aging. Adv Exp Med Biol 113:179–199.

Larkman A, Mason A. 1990. Correlations between morphology and electrophysiology of pyramidal neurons in slices of rat visual cortex I. Establishment of cell classes. J Neurosci 10:1407–1414.

Lee KF, Soares C, Beique JC. 2012. Examining form and function of dendritic spines. Neural Plast 2012:704103.

Liston C, Gan WB. 2011. Glucocorticoids are critical regulators of dendritic spine development and plasticity in vivo. Proc Natl Acad Sci U S A 108:16074–16079.

Liston C, Miller MM, Goldwater DS, Radley JJ, Rocher AB, Hof PR, Morrison JH, McEwen BS. 2006. Stress-induced alterations in prefrontal cortical dendritic morphology predict selective impairments in perceptual attentional set shifting. J Neurosci 26:7870–7874.

Liston C, Cichon JM, Jeanneteau F, Jia Z, Chao MV, Gan WB. 2013. Circadian glucocorticoid oscillations promote learning-dependent synapse formation and maintenance. Nat Neurosci 16:698–705.

Liu RJ, Aghajanian GK. 2008. Stress blunts serotonin- and hypocretin-evoked EPSCs in prefrontal cortex: role of corticosterone-mediated apical dendritic atrophy. Proc Natl Acad Sci U S A 105:359–364.

Lupien SJ, Lecours AR, Lussier I, Schwartz G, Nair NPV, Meany MJ. 1994. Basal cortisol levels and cognitive deficits in human aging. J Neurosci 14:2893–2903.

McEwen BS. 1998. Protective and damaging effects of stress mediators. N Engl J Med 338:171–179.

McEwen BS, Morrison JH. 2013. The brain on stress: vulnerability and plasticity of the prefrontal cortex over the life course. Neuron 79:16–29.

McIntyre CK, Power AE, Roozendaal B, McGaugh JL. 2003. Role of the basolateral amygdala in memory consolidation. Ann N Y Acad Sci 985:273–293.

McKlveen JM, Myers B, Flak JN, Bundzikova J, Solomon MB, Seroogy KB, Herman JP. 2013. Role of prefrontal cortex glucocorticoid receptors in stress and emotion. Biol Psychiatry 74:672–679.

Michelsen KA, van den Hove DL, Schmitz C, Segers O, Prickaerts J, Steinbusch HW. 2007. Prenatal stress and subsequent exposure to chronic mild stress influence dendritic spine density and morphology in the rat medial prefrontal cortex. BMC Neurosci 8:107.

Miller GE, Chen E, Zhou ES. 2007. If it goes up, must it come down? Chronic stress and the hypothalamic–pituitary–adrenocortical axis in humans. Psychol Bull 133:25–45.

Mitra R, Sapolsky RM. 2008. Acute corticosterone treatment is sufficient to induce anxiety and amygdaloid dendritic hypertrophy. Proc Natl Acad Sci U S A 105:5573–5578.

Mitra R, Jadhav S, McEwen BS, Vyas A, Chattarji S. 2005. Stress duration modulates the spatiotemporal patterns of spine formation in the basolateral amygdala. Proc Natl Acad Sci U S A 102:9371–9376.

Mizoguchi K, Yuzurihara M, Ishige A, Sasaki H, Chui D, Tabira T. 2000. Chronic stress induces impairment of spatial working memory because of prefrontal dopaminergic dysfunction. J Neurosci 20:1568–1574.

Mizoguchi K, Ikeda R, Shoji H, Tanaka Y, Maruyama W, Tabira T. 2009. Aging attenuates glucocorticoid negative feedback in rat brain. Neuroscience 159:259–270.

Morales-Medina JC, Sanchez F, Flores G, Dumont Y, Quirion R. 2009. Morphological reorganization after repeated corticosterone administration in the hippocampus, nucleus accumbens, and amygdala in the rat. J Chem Neuroanat 38:266–272.

Perez-Cruz C, Muller-Keuker JI, Heilbronner U, Fuchs E, Flugge G. 2007. Morphology of pyramidal neurons in the rat prefrontal cortex: lateralized dendritic remodeling by chronic stress. Neural Plast 2007:46276.

Pyter LM, Reader BF, Nelson RJ. 2005. Short photoperiods impair spatial learning and alter hippocampal dendritic morphology in adult male white-footed mice (*Peromyscus leucopus*). J Neurosci 25:4521–4526.

Radley JJ, Sisti HM, Hao J, Rocher AB, McCall T, Hof PR, McEwen BS, Morrison JH. 2004. Chronic behavioral stress induces apical dendritic reorganization in pyramidal neurons of the medial prefrontal cortex. Neuroscience 125:1–6.

Radley JJ, Rocher AB, Janssen WG, Hof PR, McEwen BS, Morrison JH. 2005. Reversibility of apical dendritic retraction in the rat medial prefrontal cortex following repeated stress. Exp Neurol 196:199–203.

Radley JJ, Rocher AB, Miller M, Janssen WG, Liston C, Hof PR, McEwen BS, Morrison JH. 2006. Repeated stress induces dendritic spine loss in the rat medial prefrontal cortex. Cereb Cortex 16:313–320.

Radley JJ, Rocher AB, Rodriguez A, Ehlenberger DB, Dammann M, McEwen BS, Morrison JH, Wearne SL, Hof PR. 2008. Repeated stress alters dendritic spine morphology in the rat medial prefrontal cortex. J Comp Neurol 507:1141–1150.

Radley JJ, Anderson RM, Hamilton BA, Alcock JA, Romig-Martin SA. 2013. Chronic stress-induced alterations of dendritic spine subtypes predict functional decrements in an hypothalamo–pituitary–adrenal-inhibitory prefrontal circuit. J Neurosci 33:14379–14391.

Radley JJ, Anderson RM, Cosme CV, Glanz RM, Miller MC, Romig-Martin SA, LaLumiere RT. 2015. The contingency of cocaine administration accounts for structural and functional medial prefrontal deficits and increased adrenocortical activation. J Neurosci 35:11897–11910.

Rodriguez A, Ehlenberger DB, Hof PR, Wearne SL. 2006. Rayburst sampling, an algorithm for automated three-dimensional shape analysis from laser scanning microscopy images. Nat Protoc 1:2152–2161.

Rodriguez A, Ehlenberger DB, Dickstein DL, Hof PR, Wearne SL. 2008. Automated three-dimensional detection and shape classification of dendritic spines from fluorescence microscopy images. PLoS One 3:e1997.

Rodriguez A, Ehlenberger DB, Hof PR, Wearne SL. 2009. Three-dimensional neuron tracing by voxel scooping. J Neurosci Methods 184:169–175.

Sapolsky RM. 1992. Do glucocorticoid concentrations rise with age in the rat? Neurobiol Aging 13:171–174.

Seib LM, Wellman CL. 2003. Daily injections alter spine density in rat medial prefrontal cortex. Neurosci Lett 337: 29–32.

Sesack SR, Deutch AY, Roth RH, Bunney BS. 1989. Topographical organization of the effect projections of the medial prefrontal cortex in the rat: an anterograde tract-tracing study with *Phaseolus vulgaris* leucoagglutinin. J Comp Neurol 290:213–242.

Shansky RM, Hamo C, Hof PR, McEwen BS, Morrison JH. 2009. Stress-induced dendritic remodeling in the prefrontal cortex is circuit specific. Cereb Cortex 19:2479–2484.

Shors TJ, Weiss C, Thompson RF. 1992. Stress-induced facilitation of classical conditioning. Science 257:537–539.

Sousa N, Lukoyanov NV, Madeira MD, Almeida OF, Paula-Barbosa MM. 2000. Reorganization of the morphology of hippocampal neurites and synapses after stress-induced damage correlates with behavioral improvement. Neuroscience 97:253–266.

Swanson AM, Shapiro LP, Whyte AJ, Gourley SL. 2013. Glucocorticoid receptor regulation of action selection and prefrontal cortical dendritic spines. Commun Integr Biol 6: e26068.

Tanokashira D, Morita T, Hayashi K, Mayanagi T, Fukumoto K, Kubota Y, Yamashita T, Sobue K. 2012. Glucocorticoid suppresses dendritic spine development mediated by downregulation of caldesmon expression. J Neurosci 32: 14583–14591.

Tiemensma J, Biermasz NR, Middelkoop HA, van der Mast RC, Romijn JA, Pereira AM. 2010a. Increased prevalence of psychopathology and maladaptive personality traits after long-term cure of Cushing's disease. J Clin Endocrinol Metab 95:E129–E141.

Tiemensma J, Kokshoorn NE, Biermasz NR, Keijser BJ, Wassenaar MJ, Middelkoop HA, Pereira AM, Romijn JA. 2010b. Subtle cognitive impairments in patients with long-term cure of Cushing's disease. J Clin Endocrinol Metab 95:2699–2714.

Tsiola A, Hamzei-Sichani F, Peterlin Z, Yuste R. 2003. Quantitative morphologic classification of layer 5 neurons from mouse primary visual cortex. J Comp Neuro 461:415–428.

van Aerde KI, Feldmeyer D. 2015. Morphological and physiological characterization of pyramidal neuron subtypes in rat medial prefrontal cortex. Cereb Cortex 25:788–805.

Vertes RP. 2004. Differential projections of the infralimbic and prelimbic cortex in the rat. Synapse 51:32–58.

Vogt BA, Peters A. 1981. Form and distribution of neurons in rat cingulate cortex: areas 32, 24, and 29. J Comp Neurol 195:603–625.

Vyas A, Mitra R, Shankaranarayana Rao BS, Chattarji S. 2002. Chronic stress induces contrasating pateterns of dendritic remodeling in hippocampal and amygdaloid neurons. J Neurosci 22:6810–6818.

Vyas A, Jadhav S, Chattarji S. 2006. Prolonged behavioral stress enhances synaptic connectivity in the basolateral amygdala. Neuroscience 143:387–393.

Watanabe Y, Gould E, Cameron HA, Daniels DC, McEwen BS. 1992a. Phenytoin prevents stress- and corticosterone-induced atrophy of CA3 pyramidal neurons. Hippocampus 2:431–435.

Watanabe Y, Gould E, McEwen BS. 1992b. Stress induces atrophy of apical dendrites of hippocampal CA3 pyramidal neurons. Brain Res 588:341–345.

Wellman CL. 2001. Dendritic reorganization in pyramidal neurons in medial prefrontal cortex after chronic corticosterone administration. J Neurobiol 49:245–253.

Wosiski-Kuhn M, Erion JR, Gomez-Sanchez EP, Gomez-Sanchez CE, Stranahan AM. 2014. Glucocorticoid receptor activation impairs hippocampal plasticity by suppressing BDNF expression in obese mice. Psychoneuroendocrinology 42: 165–177.

Yang G, Pan F, Gan WB. 2009. Stably maintained dendritic spines are associated with lifelong memories. Nature 462:920–924.

Yasumatsu N, Matsuzaki M, Miyazaki T, Noguchi J, Kasai H. 2008. Principles of long-term dynamics of dendritic spines. J Neurosci 28:13592–13608.

Yuen EY, Liu W, Karatsoreos IN, Feng J, McEwen BS, Yan Z. 2009. Acute stress enhances glutamatergic transmission in prefrontal cortex and facilitates working memory. Proc Natl Acad Sci U S A 106:14075–14079.